DEEP-Theory Meeting 14 April 2017

GALFIT and clump analysis of VELA simulations and comparison with observations — VivianTang, Yicheng Guo, David Koo

Deep Learning for Galaxies project: Analysis of VELA Gen3 simulations is ongoing by Christoph Lee and Sean Larkin, along with Avishai's student Tomer Nussbaum. Christoph is also using the DL code that classified CANDELS images to classify VELA mock galaxy images. Fernando Caro is analyzing Horizon simulations. Elliot Eckholm might be able to help visualize the VELA simulations, and Dominic Pasquale may use DL for a project to improve distance and local environment estimates for galaxies with only photometric redshifts

Circumgalactic medium (CGM): VELA mock quasar absorption spectra compared with observations - Clayton Strawn. Hassen Yesuf is working with X Prochaska to look at evidence for outflows in galaxies at z ~ 0.5 and compare with our ART simulations

Galaxy R_{eff} predicted by (spin parameter)(halo radius) = λR_{halo} paper led by Rachel Somerville — after correcting h^{-1} error, the offset between $R_{3D}/(\lambda R_{halo})$ at $z \sim 0$ and higher z has disappeared

Galaxy size vs. local density project — Christoph Lee, Graham Vanbenthuysen, Viraj Pandya, Doug Hellinger, David Koo

Improved Santa Cruz Semi-Analytic Model of galaxy population evolution — Viraj Pandya, Christoph Lee, Rachel Somerville, Sandy Faber

DM halo mass loss and **halo radial profile** papers being drafted — Christoph Lee, Doug Hellinger

Halo properties like concentration, accretion history, and spin are mainly determined by environmental density rather than by location within the cosmic web — Tze Goh, Christoph Lee, Peter Behroozi, Doug Hellinger, Miguel Aragon Calvo, Elliot Eckholm

GALFIT and clump analysis of VELA simulations and comparison with observations — VivianTang, Yicheng Guo, David Koo

Mark Mozena PhD Thesis http://physics.ucsc.edu/~joel/MOZENA_Thesis_submitted30Dec2013.pdf

Chapter 2: Comparison of Hydro-ART Simulated Galaxies with Observations

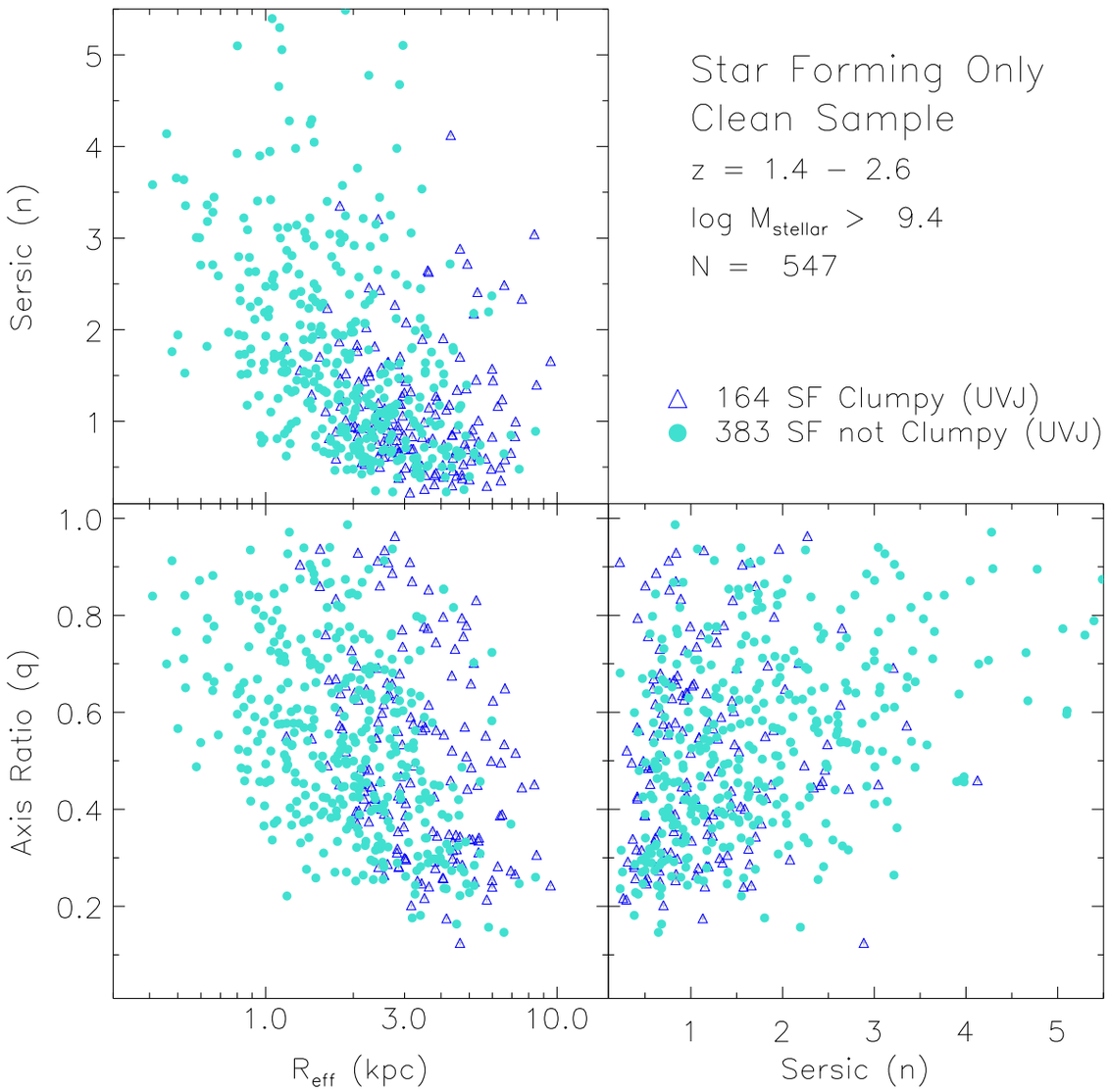

Figure 2.11: Clumpy Star-Forming GOODS-South Galaxies. 30% of z∼2 star-forming galaxies are clumpy. These clumpy systems tend to have larger R_{eff} and lower Sérsic indices.

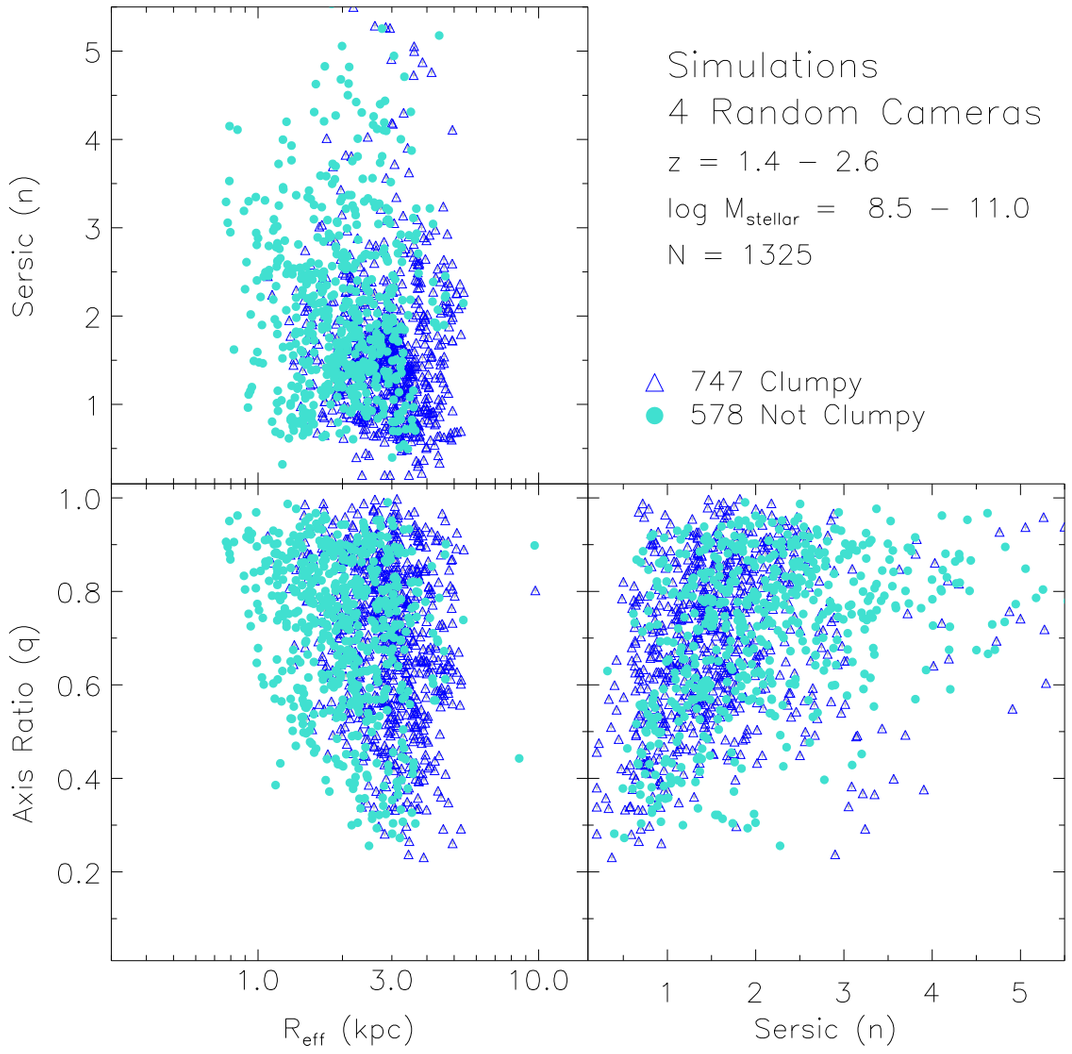

Figure 2.12: Clumpy Hydro-ART Simulations. 56% of the full Hydro-ART sample are clumpy (nearly twice the fraction seen in GOODS-South observations). As was true for the GOODS-South galaxies, the clumpy simulation galaxies are systems with larger R_{eff} and lower Sérsic indices.

Deep Learning for Galaxies project: Analysis of VELA Gen3 simulations is ongoing by Christoph Lee and Sean Larkin, along with Avishai's student Tomer Nussbaum. Christoph is also using the DL code that classified CANDELS images to classify VELA mock galaxy images. Fernando Caro is analyzing Horizon simulations. Elliot Eckholm might be able to help visualize the VELA simulations, and Dominic Pasquale may use DL for a project to improve distance and local environment estimates for galaxies with only photometric redshifts

Stochastic Order Redshift Technique (SORT): a simple, efficient and robust method to improve cosmological redshift measurements

Nicolas Tejos, Aldo Rodríguez-Puebla and Joel R. Primack, submitted to MNRAS

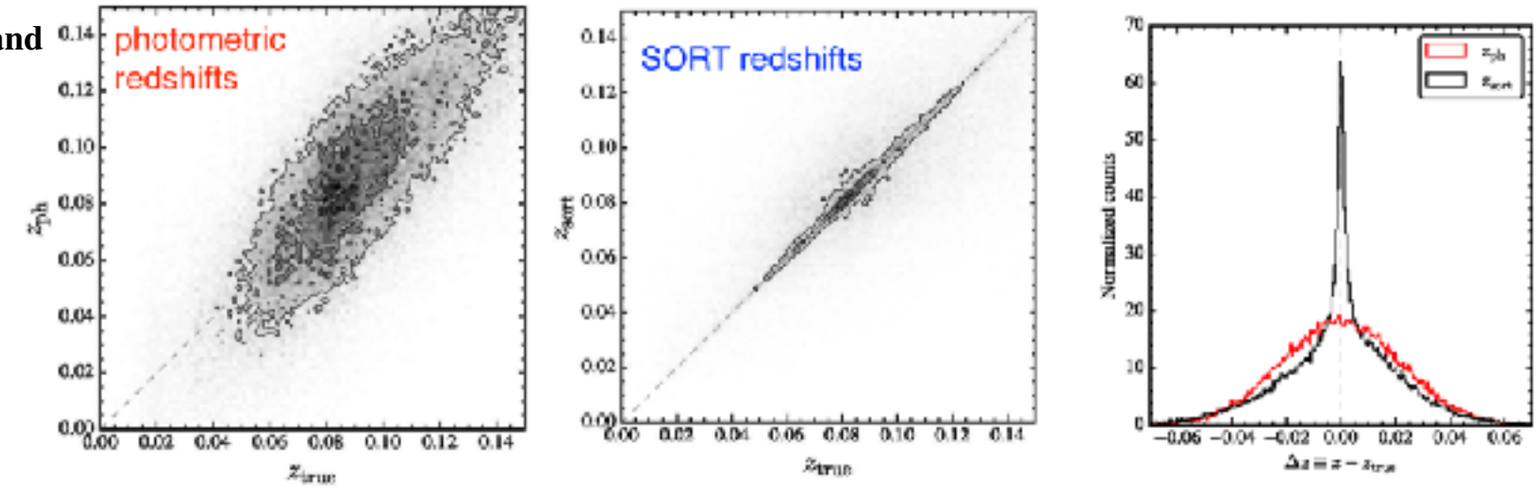

Circumgalactic medium (CGM): VELA mock quasar absorption spectra compared with observations - Clayton Strawn. Hassen Yesuf is working with X Prochaska to look at evidence for **outflows** in galaxies at z ~ 0.5 and compare with our ART simulations

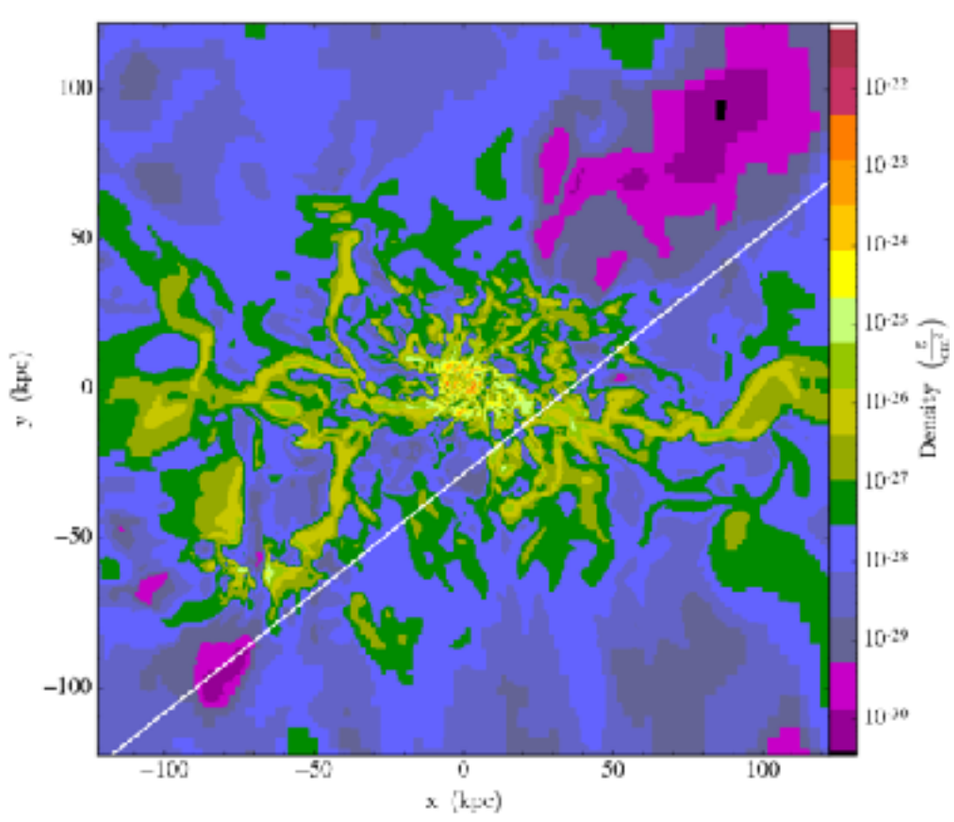

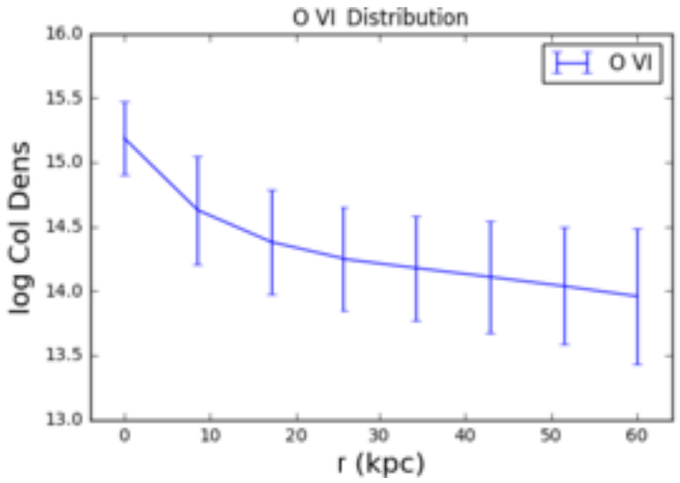

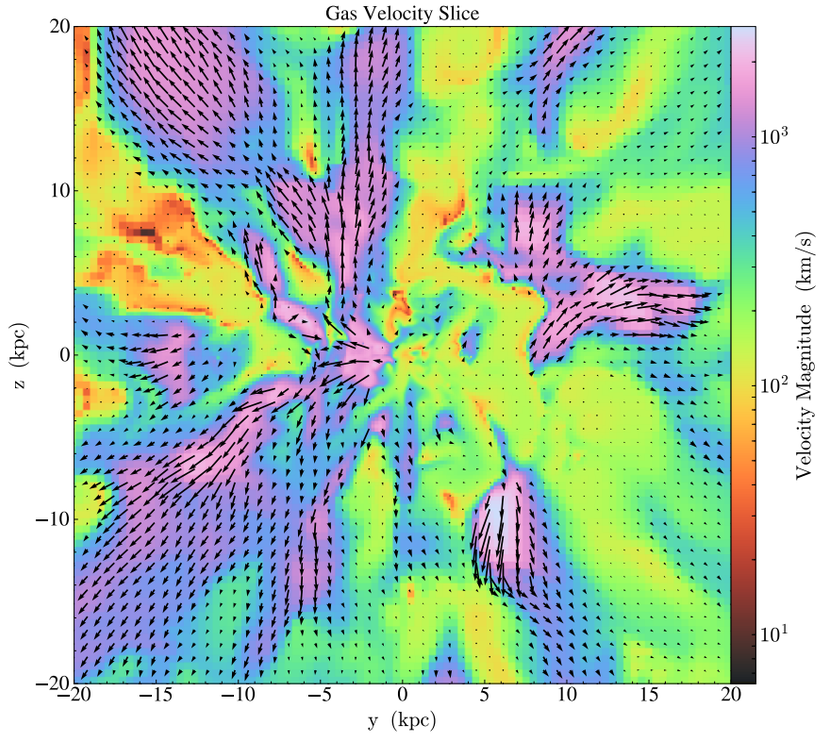

SORT allows recovery of the 2-point correlation function for $s > 4$ Mpc/h

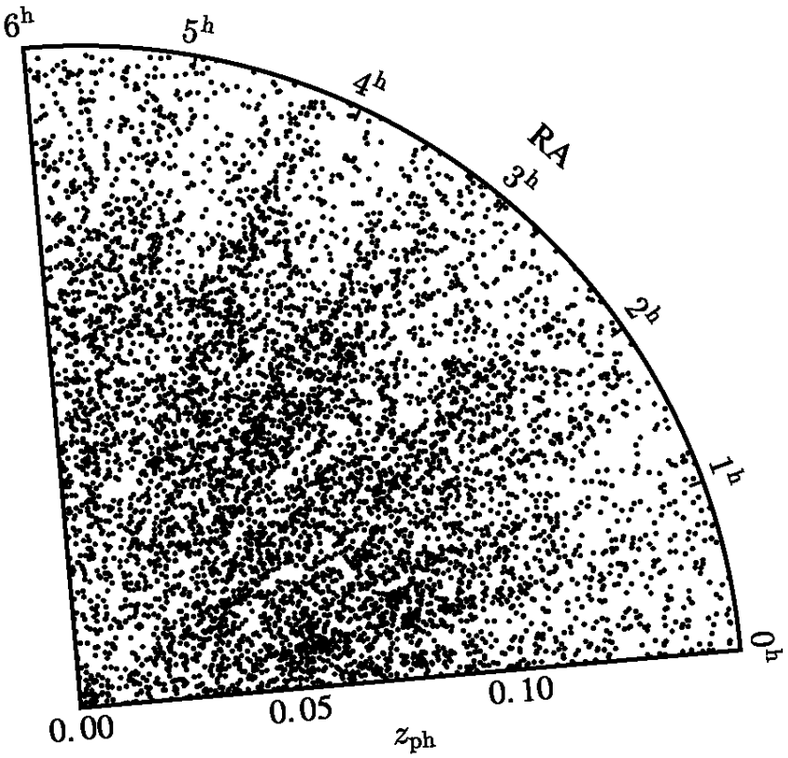

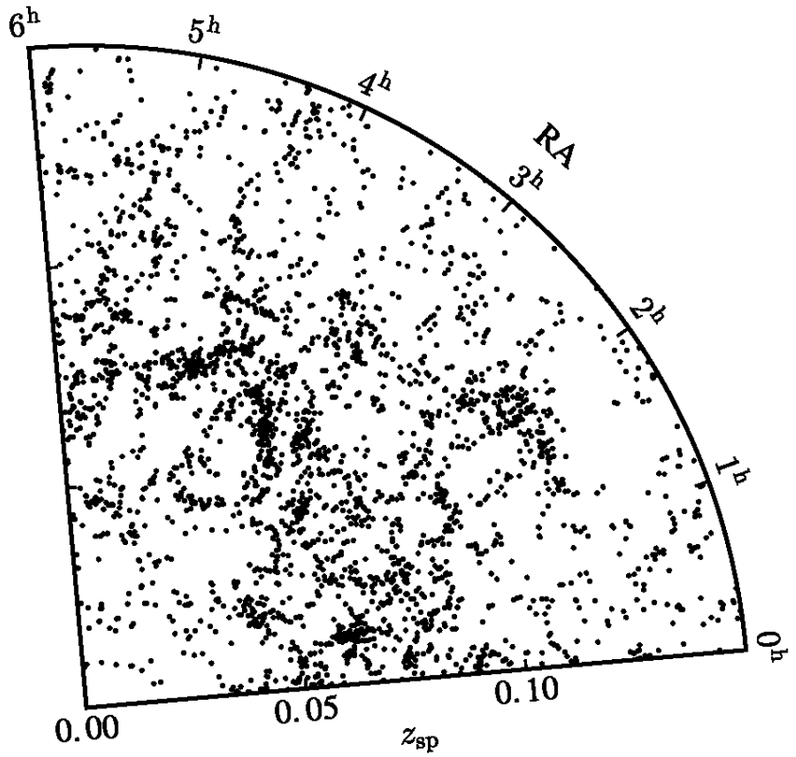

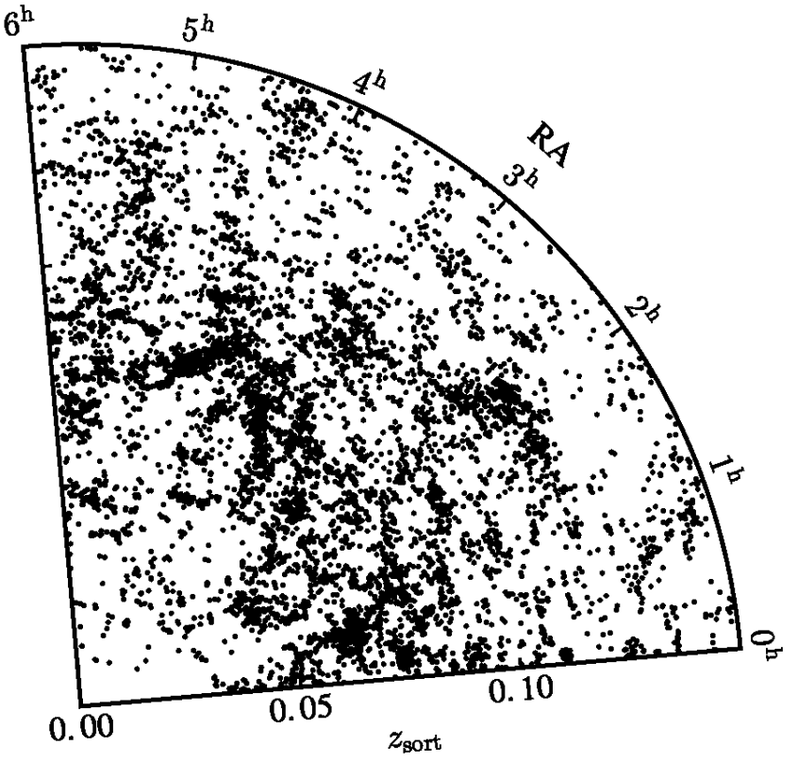

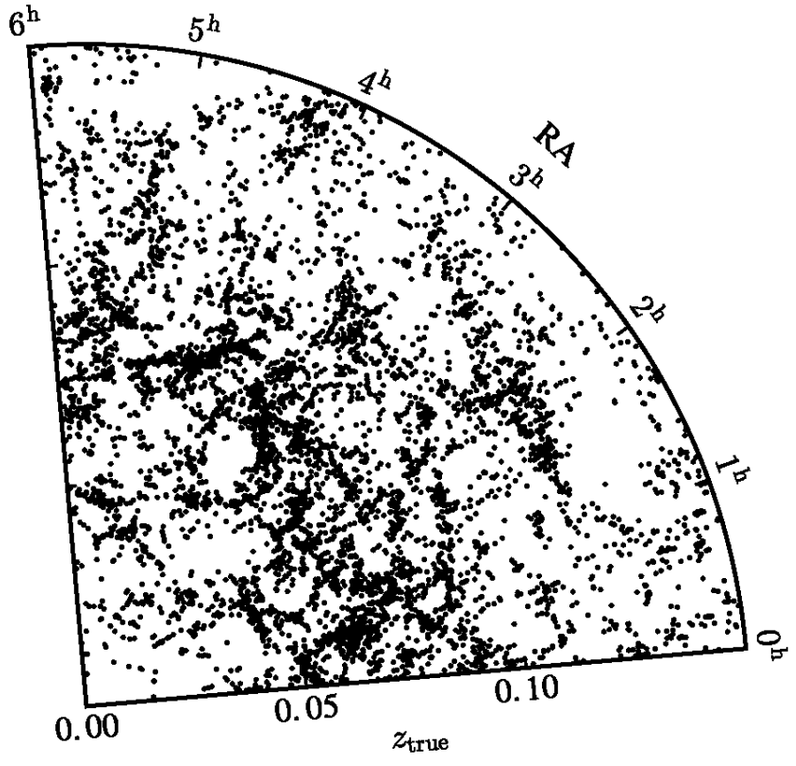

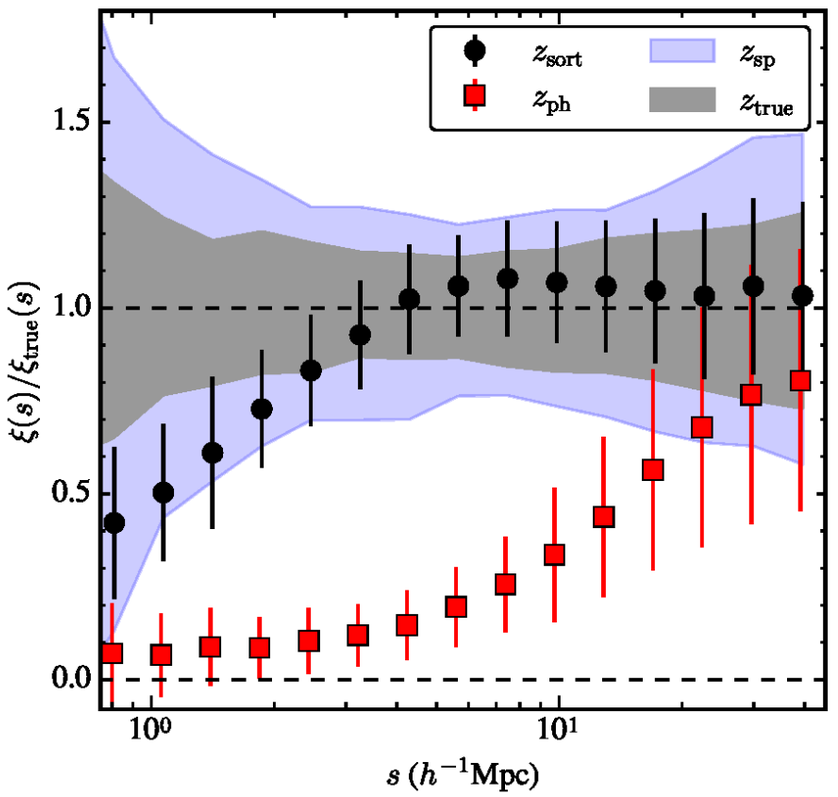

Figure 7. The ratio between the measured redshift-space two-point correlation function and its underlying true value, $\xi(s)/\xi_{\rm true}(s)$, as a function of redshift space distance s. The black circles correspond to using $z_{\rm sort}$ and the red squares correspond to using $z_{\rm ph}$ (slightly offset in the x-axis for clarity). Uncertainties were estimated from a bootstrap technique from 100 realizations. The grey shaded area corresponds to the intrinsic 1σ uncertainty limit due to sample variance (i.e. this is the uncertainty assuming we knew the underlying true redshift for all the galaxies in the original photometric sample). The light-blue area corresponds to the 1σ uncertainty around the unbiased $z_{\rm sp}$ measurement from the spectroscopic sample (i.e. the remaining 30% of galaxies used as reference). See Section 4.3.2 for further details.

Galaxy size vs. local density project — Christoph Lee, Graham Vanbenthuysen, Viraj Pandya, Doug Hellinger, David Koo

Doug recommended that we use Delaunay tessellation method to estimate density around SDSS galaxies

Voronoi tessellation

Delaunay tessellation is dual to Voronoi tessellation

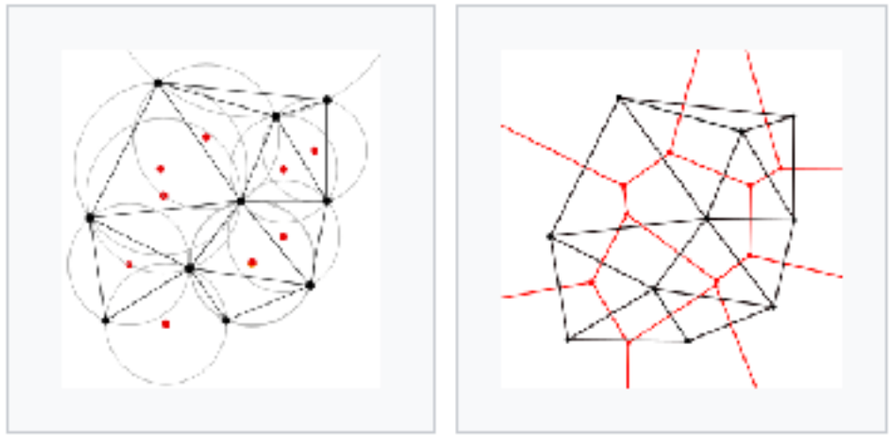

The Delaunay triangulation with all the circumcircles and their centers (in red).

Connecting the centers of the circumcircles produces the Voronoi diagram (in red).

The DTFE public software

-The Delaunay Tessellation Field Estimator code -

Marius Cautun, Rien van de Weygaert

arXiv:1105.0370

We present the DTFE public software, a code for reconstructing fields from a discrete set of samples/measurements using the maximum of information contained in the point distribution. The code is written in C++ using the CGAL[1] library and is parallelized using OpenMP. The software was designed for the analysis of cosmological data but can be used in other fields where one must interpolate quantities given at a discrete point set. The software comes with a wide suite of options to facilitate the analysis of 2- and 3-dimensional data and of both numerical simulations and galaxy redshift surveys. For comparison purposes, the code also implements the TSC and SPH grid interpolation methods. The code comes with an extensive user guide detailing the program options, examples and the inner workings of the code. The DTFE public software and further information can be found at http://www.astro.rug.nl/∼voronoi/DTFE/dtfe.html.

Galaxy $R_{\rm eff}$ predicted by (spin parameter)(halo radius) = $\lambda R_{\rm halo}$ paper led by Rachel Somerville — after correcting h^{-1} error, the offset between $R_{\rm 3D}/(\lambda R_{\rm halo})$ at $z \sim 0$ and higher z has disappeared

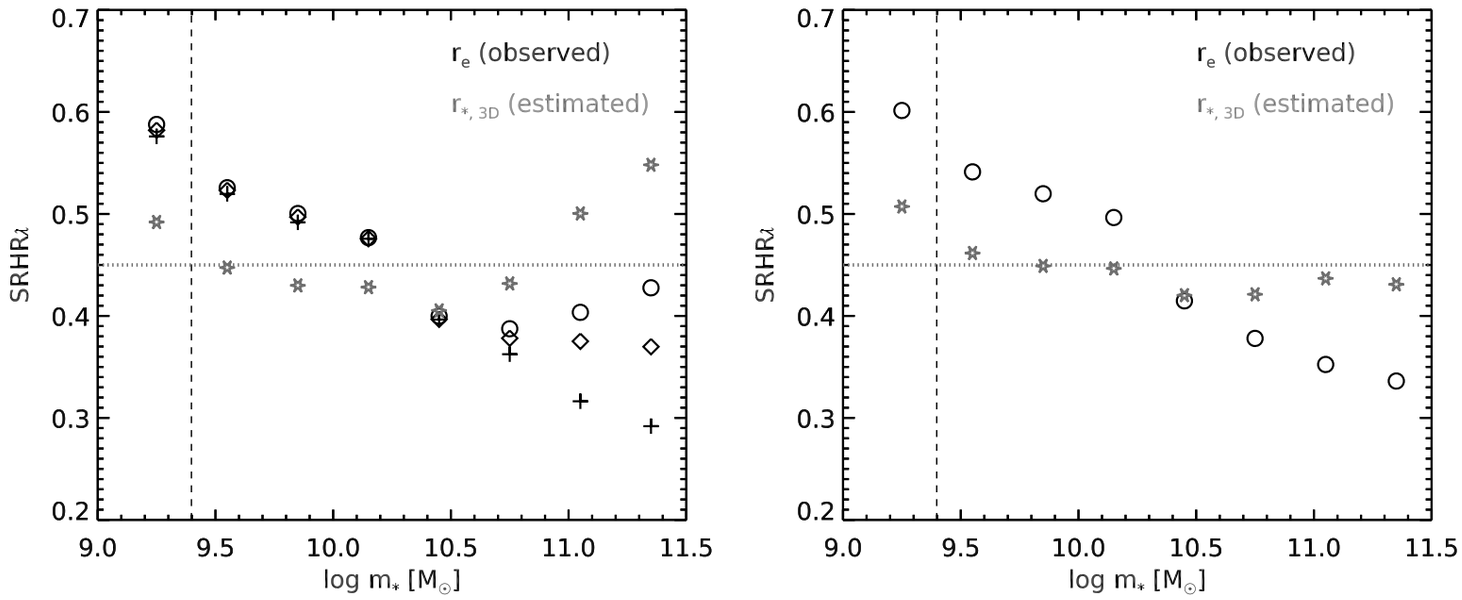

Figure 2. Median galaxy radius divided by the median value of the spin parameter times the halo virial radius, in bins of stellar mass, at $z \sim 0.1$. **Left panel: New results using B17 SMHM relation.** Open circles are based on the GAMA DR2 catalogs and are for the observed (projected) r-band half-light radius r_e. The dashed vertical line shows the 97.7% stellar mass completeness limit for the GAMA sample. Gray star symbols show the same quantity for the estimated 3D half-stellar mass radius ($r_{*,\rm 3D}$). Crosses show the observed (projected) SRHRλ where no scatter is included in the SMHM relation, and diamonds show results with a reduced intrinsic scatter of $\sigma_{\rm int} = 0.16$ dex instead of the fiducial value of 0.22 dex. **Right panel: plot from submitted paper, which used B13 with an intrinsic scatter of 0.15 dex and did not include scatter from stellar mass errors.**

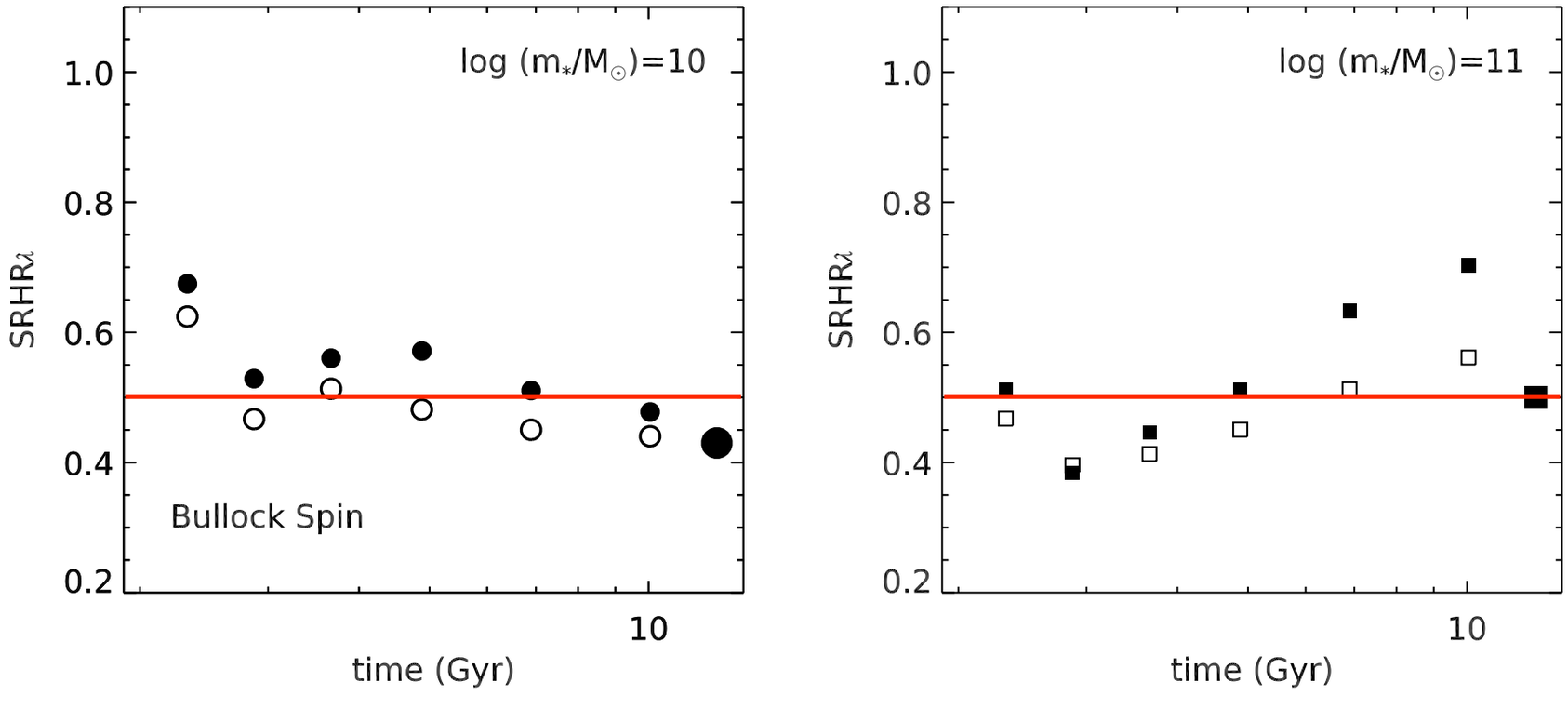

The Astrophysical Journal Letters, 764:L31 2013 February 20

Andrey V. Kravtsov: THE SIZE–VIRIAL RADIUS RELATION OF GALAXIES

ABSTRACT

I use the abundance matching ansatz, which has proven to be successful in reproducing galaxy clustering and other statistics, to derive estimates of the virial radius, R_{200}, for galaxies of different morphological types and a wide range of stellar masses. I show that over eight orders of magnitude in stellar mass galaxies of all morphological types follow an approximately linear relation between half-mass radius of their stellar distribution, $r_{1/2}$, and virial radius, $r_{1/2} \approx 0.015\,R_{200}$, with scatter of $\approx$0.2 dex. Such scaling is in remarkable agreement with the expectation of models that assume that galaxy sizes are controlled by halo angular momentum, $r_{1/2} \propto \lambda R_{200}$, where λ is the spin of galaxy parent halo. The scatter about the relation is comparable with the scatter expected from the distribution of λ. Moreover, I show that when the stellar and gas surface density profiles of galaxies of different morphological types are rescaled by the radius $r_n = 0.015\,R_{200}$, the rescaled profiles follow approximately universal exponential (for late types) and de Vaucouleurs (for early types) form with scatter of only $\approx$30%–50% at $R \approx 1$–$3r_n$. Remarkably, both late- and early-type galaxies have similar mean stellar surface density profiles at $R \gtrsim 1r_n$. The main difference between their stellar distributions is thus at $R < r_n$. The results of this study imply that galaxy sizes and radial distribution of baryons are shaped primarily by properties of their parent halos and that the sizes of both late-type disks and early-type spheroids are controlled by halo angular momentum.

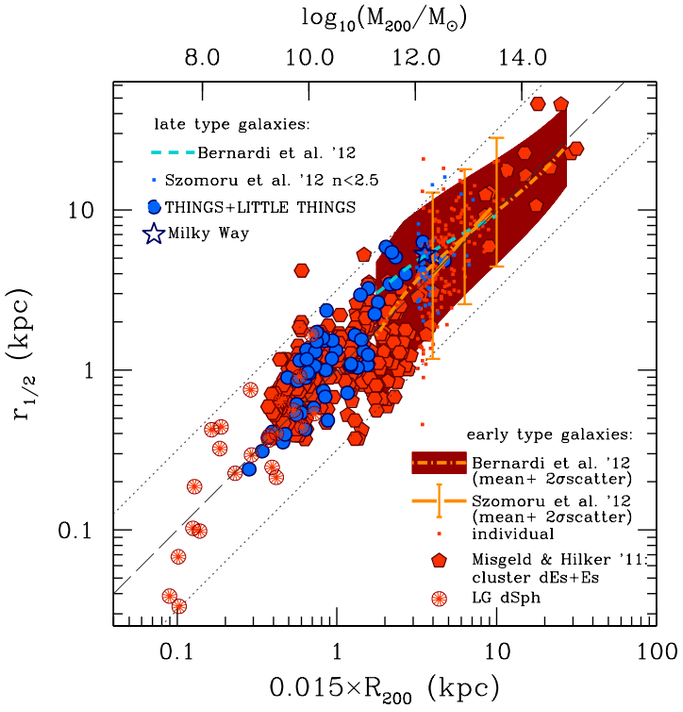

Figure 1. Relation between the half-mass radius of stellar distribution in galaxies of different stellar masses (spanning more than eight orders of magnitude in stellar mass) and morphological types and inferred virial radius of their parent halos, R_{200}, defined as the radius enclosing overdensity of $200\rho_{\rm cr}$, and estimated as described in Section 2. The red and orange symbols and lines show early-type galaxies, while blue and cyan symbols and line show late-type galaxies, as indicated in the figure legend (see Sections 3 and 4.1 for details). The gray dashed line shows linear relation $r_{1/2} = 0.015\,R_{200}$ and dotted lines are linear relations offset by 0.5 dex, which approximately corresponds to the 2σ scatter $2\sigma_{\ln\lambda} \approx 1.1$ expected for dark matter halos.

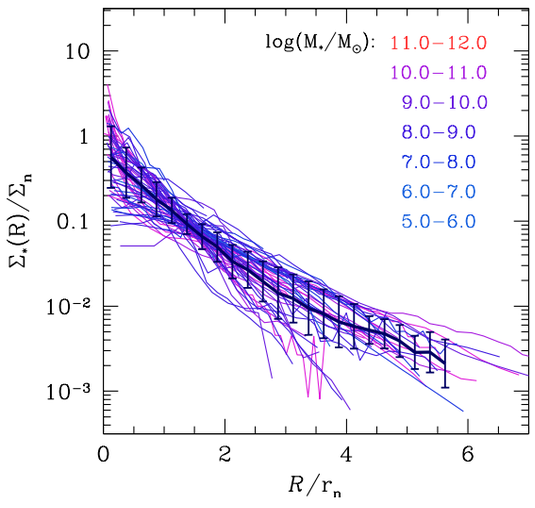

Late-type Galaxies: Stars

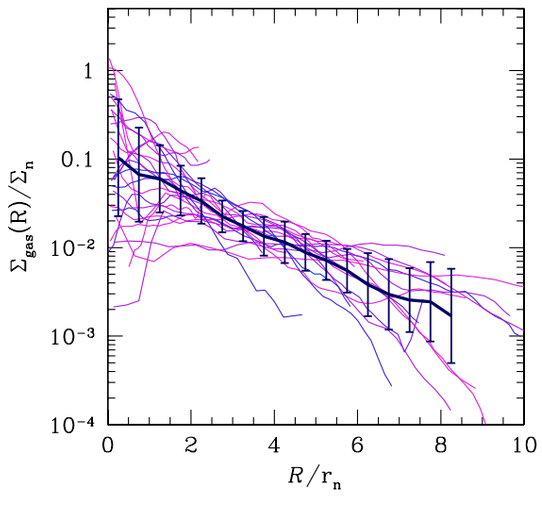

Late-type Galaxies: Gas

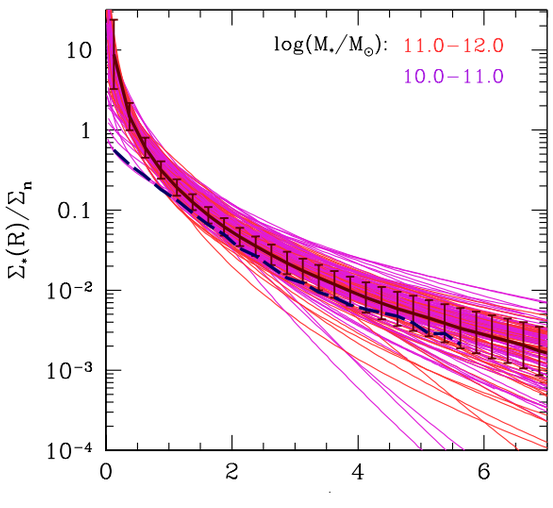

Early-type Galaxies: Stars

The thick dashed line shows the average profile of late-type galaxies from the top panel of Figure 2 for comparison.

Halo properties like concentration, accretion history, and spin are mainly determined by environmental density rather than by location within the cosmic web — Tze Goh, Christoph Lee, Peter Behroozi, Doug Hellinger, Miguel Aragon Calvo, Elliot Eckholm

Histogram distribution of SpinB of all Halos with various density ranges in various-sized walls.

Halos in ALL Environments

Halos in WALLS only

Halos in Voids

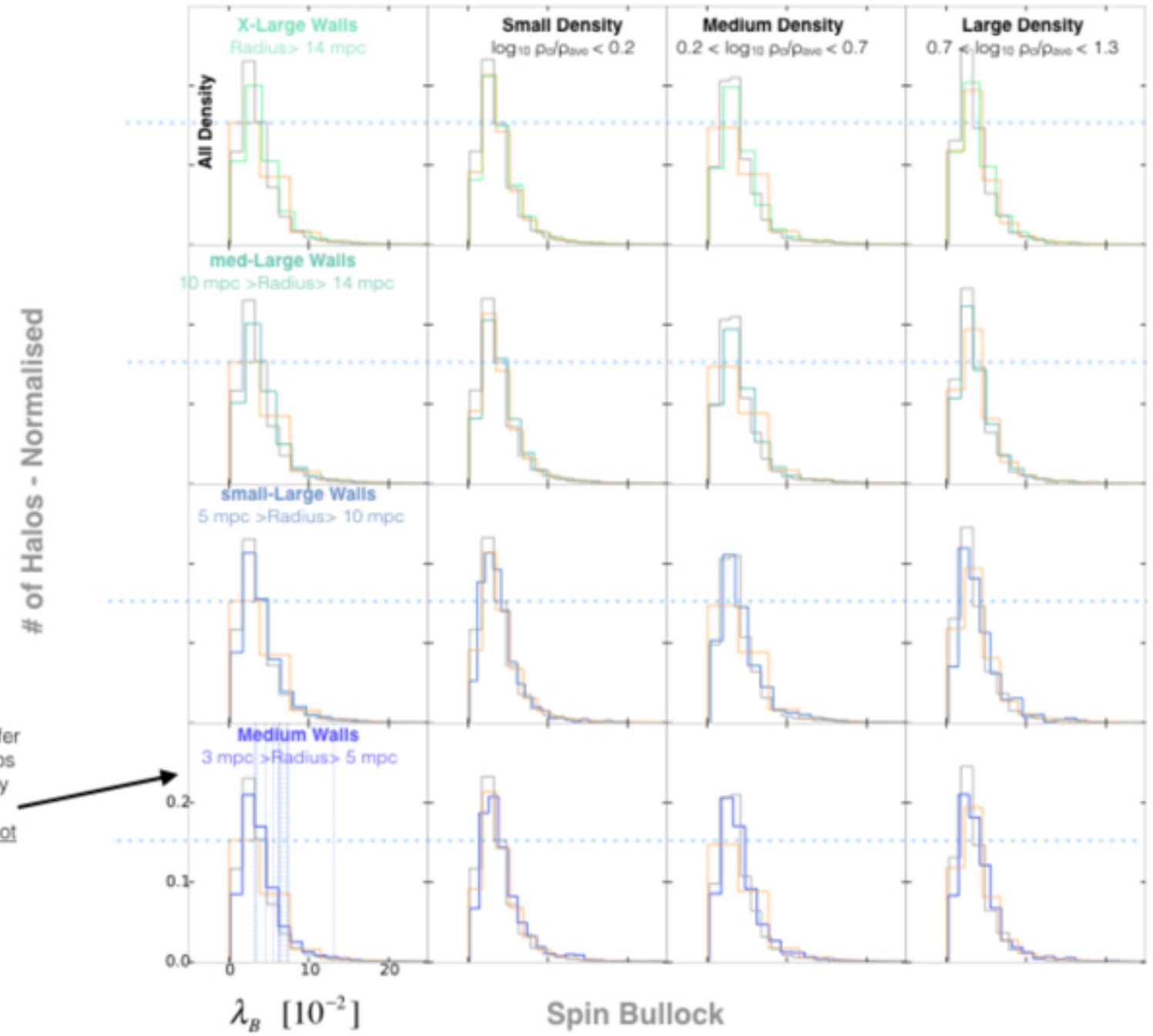

$\log_{10} M_{vir} = 11.20 \pm 0.375$

Note: Most of the Histograms have very large tails. That is, the SpinB can reach 70 , but then the histogram itself becomes unreadable

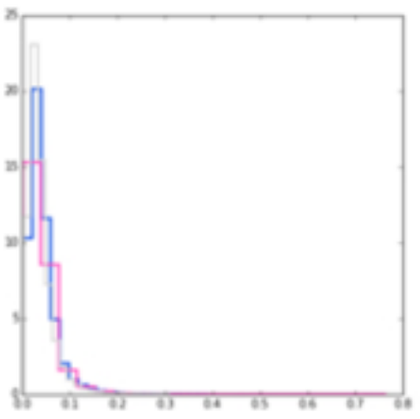

Note: Vertical blue lines refer to the Spin B of the 10 halos that are similar to the Milky Way Galaxy.
As you can see, they are <u>not</u> close to the Gaussian.

Spin Bullock vs Density

SpinB is compared with density in different mass bins of sub-Large sized walls only

Halos in ALL Environments

Halos in WALLS only

Halos in Voids